

Site-Specific Inhibition of Transcription Factor Binding to DNA by a Metallointercalator[†]

Duncan T. Odom, Carl S. Parker, and Jacqueline K. Barton*

Division of Chemistry and Chemical Engineering, California Institute of Technology, Pasadena, California 91125

Received November 25, 1998; Revised Manuscript Received February 3, 1999

ABSTRACT: The metallointercalator Λ -1-Rh(MGP)₂phi⁵⁺ binds tightly and specifically to the site 5'-CATATG-3' in the major groove of double helical DNA by a combination of direct readout and shape selection. To examine competitive interactions between this small metal complex and a DNA-binding transcription factor, the preferred binding site for Λ -1-Rh(MGP)₂phi⁵⁺ was engineered into the AP-1 recognition element (ARE) of the major-groove binding bZIP transcription factor yAP-1, the yeast analogue of mammalian AP-1. Binding experiments confirmed that the modified ARE retained normal yAP-1 binding affinity. Photocleavage experiments demonstrated that the modified ARE contained a high-affinity binding site for Λ -1-Rh(MGP)₂phi⁵⁺, whereas the native ARE showed no interaction. Competition experiments using gel shift mobility assays demonstrated that Λ -1-Rh(MGP)₂phi⁵⁺ at 120 nM competes 50% of yAP-1 binding to the 5'-CATATG-3' containing oligonucleotide. In contrast, competitive disruption of protein binding to the native ARE requires 3 μ M Λ -1-Rh(MGP)₂phi⁵⁺. Metallointercalator derivatives, including geometric isomers of Λ -1-Rh(MGP)₂phi⁵⁺, show no specific binding to the target site and show no inhibition of yAP-1/DNA complexes at concentrations as high as 20 μ M. Thus, metallointercalators can be tuned to show selectivity for major groove sites on DNA comparable to transcription factors and indeed can inhibit transcription factor binding site selectively.

Proteins that interact with DNA are the subjects of great interest in developing potential targets for therapeutic treatment. Since transcription factors modulate the expression of genes by binding to and interacting with specific DNA sequences, one frequent target for drug design and biochemical modification has been the DNA-binding sites of transcription factors. One method for altering transcription regulation both in vivo and in vitro is to modify the DNA bases of the protein binding site. Enzymatic base methylation (1), the formation of cisplatin lesions (2–4), and chemical alkylation (5, 6) have been used successfully to affect the binding of proteins to DNA. However, these covalent modifications frequently show little sequence specificity beyond that of individual base preferences. The lack of extended sequence selectivity effectively prevents targeting specific genes and functions in vivo.

Alternatively, agents which bind DNA noncovalently may be used to interfere competitively with DNA-binding proteins. One method for targeting specific genetic loci has been to use complementary protein nucleic acids (PNAs); however, these molecules may lack the cell permeability that is needed to make them effective therapeutic agents (7). The natural product calicheamicin as well as some derivatives have been shown to bind sequence selectively to the minor groove of DNA and to inhibit transcription factor binding (8–10); calicheamicin in vivo cleaves the sugar phosphate backbone of DNA.

Another particularly promising class of potential therapeutics is the polyamides. These small synthetic molecules bind to DNA in the minor groove with high sequence specificity (11) and have been shown to inhibit transcription both in vitro and in vivo (12). Often in conjunction with major groove contacts, the minor groove is contacted by many transcription factors. By disrupting the minor groove contacts, a number of transcription factors can be displaced.

Currently, however, few strategies exist that utilize the major groove directly as a surface for recognition by small molecules to inhibit the initiation of transcription. Because the major groove is preferentially recognized by transcription factors (7), small molecules that recognize specified regions within the major groove might be especially effective in blocking DNA binding. The steric accessibility of the wide and deep major groove, the greater range of functionality within the major groove versus the minor groove, and the possibility of cooperative, multiple protein–DNA contacts in the major groove make it an attractive target for therapeutic design. Hence, it would be of great interest to find a class of small molecules that can competitively inhibit the binding of transcription factors in the major groove.

Our research has focused on the development of metallointercalators that bind to DNA in the major groove (13, 14). Phenanthrenequinone diimine (phi) complexes of rhodium, such as Rh(phen)₂phi³⁺ and Δ - α -[Rh[(R,R)-Me₂trien]phi]³⁺ (Me₂trien=2,9-diamino-4,7-diazadecane) are octahedral complexes which are coordinatively saturated and inert to ligand substitution. The phi ligand, an extended aromatic, heterocyclic surface, preferentially intercalates between the DNA base pairs, and in so doing, the intercalated phi orients the

[†] We are grateful to the NIH (GM33309 to J.K.B. and GM47381 to C.S.P.) for their financial support and for an NRSA traineeship to D.T.O.

* To whom correspondence should be addressed.

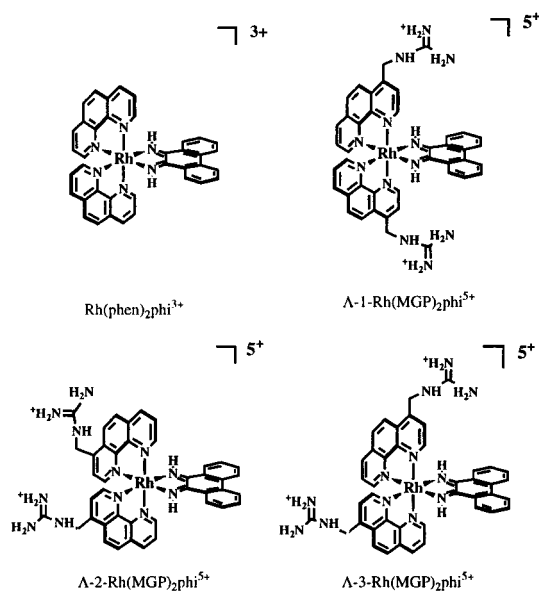


FIGURE 1: Λ isomers of metal complexes used in competition experiments. The parent compound $\text{Rh}(\text{phen})_2\text{phi}^{3+}$ is an intercalator that binds with relative sequence neutrality and approaches the base stack from the major groove. The isomers of the metal complex based on methylguanidinium phenanthroline (MGP) are additionally shown. 1- $\text{Rh}(\text{MGP})_2\text{phi}^{5+}$ positions guanidiniums above the intercalating ligand, and directed toward the DNA base stack. This positioning affords it strong, selective recognition of its 5'-CATATG-3' target. 2- $\text{Rh}(\text{MGP})_2\text{phi}^{5+}$ positions the guanidiniums away from the base stack, thereby removing them from contact with functional groups on the DNA, and making this complex relatively nonspecific in its recognition, similar to the parent compound $\text{Rh}(\text{phen})_2\text{phi}^{3+}$. 3- $\text{Rh}(\text{MGP})_2\text{phi}^{5+}$ shows limited recognition of the same sites as 1- $\text{Rh}(\text{MGP})_2\text{phi}^{5+}$.

rigid complex with respect to the helix. All phi complexes of rhodium examined thus far appear to intercalate into the major groove side of the DNA duplex (13–17). The ancillary ligands of these phi complexes can be tuned to provide sequence specificity through the geometrical positioning of functional groups on the ligands relative to the DNA bases to create an ensemble of sequence-determining interactions in the major groove. One well-characterized example of predictive design utilizing this idea has been the metallo-intercalator $\Delta\text{-}\alpha\text{-}[\text{Rh}[(\text{R},\text{R})\text{-Me}_2\text{trien}]\text{phi}]^{3+}$. This complex recognizes its target site 5'-TGCA-3' through a mixture of hydrogen-bonding interactions between the axial amines of the complex and guanine bases and van der Waals contacts between methyl groups on the ligands and on the thymine residues positioned in the major groove (15, 18). In addition, upon irradiation with ultraviolet light of the phi complexes of rhodium bound to DNA, direct DNA strand scission occurs in a reaction consistent with radical abstraction of a sugar hydrogen; this photochemistry is useful in marking sites of specific binding by the complex on DNA (19).

Here, our focus is on phi complexes of rhodium that have functionalized phenanthrolines as ancillary ligands (Figure 1). These complexes have been shown to exploit a combination of direct readout and shape selectivity to recognize sites in DNA (13, 20). The parent complex of this series is $\text{Rh}(\text{phen})_2\text{phi}^{3+}$, which recognizes sites, notably 5'-pyrimidine-purine-3' steps, based upon shape selection (19, 21). The sites recognized are those which are somewhat more open in the major groove relative to B-form DNA. These openings better accommodate the large ligand array displayed by Rh -

$(\text{phen})_2\text{phi}^{3+}$. Nonetheless, this shape selectivity provides only a small amount of sequence selectivity.

The pendant guanidiniums on the ancillary phenanthroline rings of $\text{Rh}(\text{MGP})_2\text{phi}^{5+}$ (MGP = 4-guanidylmethyl-1,10-phenanthroline) lead instead to a high level of DNA site specificity (Figure 1). The guanidinium groups of arginine side chains are exploited frequently by proteins in targeting guanine residues of DNA (22). Because the MGP ligand is asymmetrically functionalized, multiple regioisomers of the complex exist. There are three geometric isomers, each of which has two stereoisomers. Remarkably, each of these different isomers exhibits quite different recognition of DNA, demonstrating that the metal complex binding is dependent upon the alignment of functional groups. Notably, the symmetric isomer 2, with guanidiniums pointing away from the phi ligand, shows sequence selectivity resembling that of $\text{Rh}(\text{phen})_2\text{phi}^{3+}$.

Of particular interest, the symmetric isomer $\Lambda\text{-}1\text{-Rh}(\text{MGP})_2\text{phi}^{5+}$, with guanidinium arms that extend axially from the intercalating phi plane forward over the phi ligand, displays strong and site-selective binding to DNA. $\Lambda\text{-}1\text{-Rh}(\text{MGP})_2\text{phi}^{5+}$ binds preferentially to the site 5'-CATATG-3' with nanomolar affinity. Although there is some tolerance for differences at the outermost positions in the 6 base pair site (13), any variation of the central 5'-ATAT-3' disfavors metal complex intercalation. Molecular modeling shows that, in the absence of DNA distortion, the stereochemistry of the guanidinium groups on the complex does not permit the bases at the extremities to be contacted by the guanidiniums, yet binding experiments in which guanines were replaced with deazaguanine have shown that terminal guanine-guanidinium contacts occur. DNA cyclization assays established that the intercalation of the metal complex is associated with a 70° unwinding at the DNA site, and this unwinding explains how the positioning of guanine-guanidinium contacts can occur. NMR evidence further suggests that the metal complex traps the DNA site in an unwound form, hence the strict requirement for a central TA-rich stretch (23).

The six base pair recognition of a DNA site by this small synthetic complex, as well as the unwinding and exchange kinetics associated with binding, may resemble the interactions of many proteins that bind to DNA site specifically. Significant bend angles are often found in DNA remodeling proteins, for instance, TATA box binding protein (TBP) (24, 25). Not only is $\Lambda\text{-}1\text{-Rh}(\text{MGP})_2\text{phi}^{5+}$ similar to TBP in that it uses guanidinium functionalities to generate a network of hydrogen bonds to DNA, but with both TBP and the synthetic metal complex, significant unwinding (70° vs 108° for TBP) and kinking of the bound site occurs. Indeed, the preferential recognition of sites by TBP that contain TA-rich stretches may share mechanistic features with the targeting of $\Lambda\text{-}1\text{-Rh}(\text{MGP})_2\text{phi}^{5+}$ to its preferred binding site (13).

One of the prominent classes of proteins that site specifically interact with DNA is the bZIP transcription factors (26). Several of these proteins bound to their target DNA sites have been structurally characterized, among them is the transcription factor GCN4, and in these structures, a common structural motif is apparent. Most prominent is the dimerization domain which includes a coiled coil α -helical region stabilized by the packing of leucine side chains; the dimerization domain is capped by a highly basic, DNA-binding

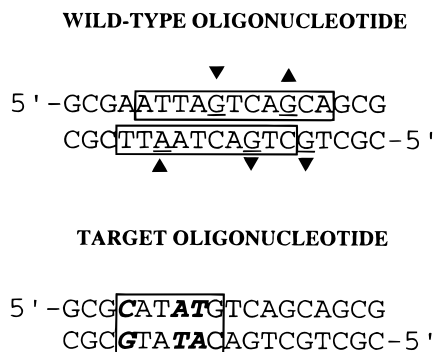


FIGURE 2: Modifications made to the ARE to incorporate a metal complex binding site (adapted from ref 14). The top oligonucleotide sequence (labeled wild-type) is the wild-type ARE, capped with GCG triplets. The boxed regions show protection against MPE footprinting in the presence of yAP-1. The solid triangles indicate increases or decreases in sensitivity in DMS labile sites when footprinted in the presence of yAP-1. The target strand, below, has incorporated a 5'-CATATG-3' site with no disruption of the footprinted nucleotides. The bases modified are shown in bold italics.

region. Separate regions either upstream or downstream of the bZIP DNA binding motif regulate transcriptional activation and signaling. Another member of this class of transcription factors is the yeast analogue of mammalian AP-1, yAP-1, which is 70 kDa in size (27). yAP-1 shows sequence homology to other bZIP transcription factors, and the isolated DNA-binding region from yAP-1 shows the induction of an α helix upon binding to its DNA recognition site, consistent with the leucine zipper motif (28). Functionally, yAP-1 regulates pleiotropic drug resistance and has been shown to be nonessential for cell viability under normal circumstances (29). yAP-1 has a strong affinity for the site 5'-AATTAGT-CAGCA-3', known as the activator recognition element (ARE). Aspects of how yAP-1 recognizes its target site have been determined by chemical probing with dimethyl sulfate (DMS), DNase I, and methidiumpropylEDTA iron digestion (MPE) (Figure 2, top sequence) (30). Footprinting with MPE suggests that the yAP-1-binding domain spans the consensus site, but DMS digestion of DNA in the presence of yAP-1 reveals that there are a number of base pairs within the core of the consensus region that do not appear to be in intimate contact with the protein. This apparent lack of contact at particular locations within the site suggested the target site could be mutated to contain an overlapping site for Λ -1-Rh(MGP)₂phi⁵⁺ without affecting the ARE specific binding of the protein. Such a DNA site would allow competitive assays to be carried out between yAP-1 and Λ -1-Rh(MGP)₂phi⁵⁺.

The notion of establishing a functional similarity between Λ -1-Rh(MGP)₂phi⁵⁺ and a DNA-binding proteins such as yAP-1 in targeting a specific site is interesting to consider in light of the much smaller size and relative simplicity of the transition metal complex. If this metal complex could be used to inhibit the binding of a protein to DNA by recognition of a common site, this reactivity would strengthen the possible application of metallointercalators as competitive agents to alter transcription. The findings reported herein demonstrate that indeed Λ -1-Rh(MGP)₂phi⁵⁺ can be used to inhibit site specifically the binding of a transcription factor to a promoter site in vitro. We show that this interaction is

dependent both on the identity of the metal complex and on the presence of a metal complex binding site.

MATERIALS AND METHODS

All chemicals and biochemicals were from commercial sources. Beckman JA2-21 and JA-4 centrifuges were used for general purposes. A Branson Sonifier 450 was used to lyse cell preparations. All enzymes were purchased from commercial sources unless otherwise noted. All proteins were stored at -20 °C in protein buffer that consisted of 10% glycerol, 25 mM hepes, pH 7.4, 1 mM EDTA, 50 mM KCl, and 0.1% Nonidet-40.

Synthesis and Purification of DNA and Metal Complexes. All DNA was synthesized with a terminal trityl group on an ABI 392 DNA/RNA synthesizer with reagents from Glen Research. HPLC purification and subsequent detritylation used standard techniques. All labeled oligonucleotides were 5'-end labeled using standard protocols with polynucleotide kinase (New England Biolabs) and γ -³²P-ATP. The labeled DNA was purified by denaturing gel electrophoresis on a 20% acrylamide gel, followed by crush and soak elution in 10 mM Tris-HCl, pH 7.4, and 1 mM EDTA. The purified labeled material was then annealed to a 10-fold excess of complement, and native gel electrophoresis performed on a 10% polyacrylamide gel containing 90 mM Tris borate, pH 8.3, and 1 mM EDTA. The synthesis and purification of the metal complexes followed previously reported procedures (20, 31).

Preparation of Recombinant yAP-1 Expression Vector. The plasmid pUC19 containing the complete open reading frame of the *YAP1* gene in 2.5 kB of yeast cDNA was digested with *EcoRI*, and the *YAP1* gene was isolated by agarose gel electrophoresis. pBluescript IISK(-) was digested with *EcoRI* and calf alkaline phosphatase, and gel purified. The previously isolated *YAP1* gene was ligated into this pBS vector, and successful ligations were selected by ampicillin resistance in DH5 α *E. Coli* cells. Plasmids from this step were harvested and inserted into CJ236 (*dut*-, *ung*-) cells. K07 helper phage and kanamycin selection was used with this construction to generate a ssDNA template for site-directed mutagenesis (32). A 3' *SalI* restriction site and a 5' *NsiI* restriction site were introduced into the *YAP1* gene. The gene was excised, isolated, and ligated into a thioredoxin fusion expression vector pThioHisA (Invitrogen). The 5' and 3' termini of pThioHis(yAP-1) were sequenced, verifying proper framing and mutagenesis.

Expression and Purification of Recombinant yAP-1 Protein. The vector pThioHis(yAP-1) was transfected into DE3 cells (BL21), and four to five colonies were selected from an LB-ampicillin plate incubated overnight at 37 °C. These colonies were used directly to infect 1 L of LB media with 40 μ g/mL ampicillin with shaking at 200 rpm at 37 °C. At OD₅₉₅ = 0.6, 10 mL of 100 mM isopropylthiogalactoside was added to a final concentration of 1 mM, and the cells were transferred to a 30 °C shaker. After 3 h of induction, the cells were harvested by 15 min centrifugation at 1000g, and frozen overnight at -80 °C. The cell pellet was rinsed with and then resuspended into 20 mL of protein buffer with 1 mM α -toluenesulfonyl fluoride. To this, 40 mg lysozyme was added, and the solution was incubated at 23 °C for 20 min. This solution was then sonicated at 50% duty cycle for

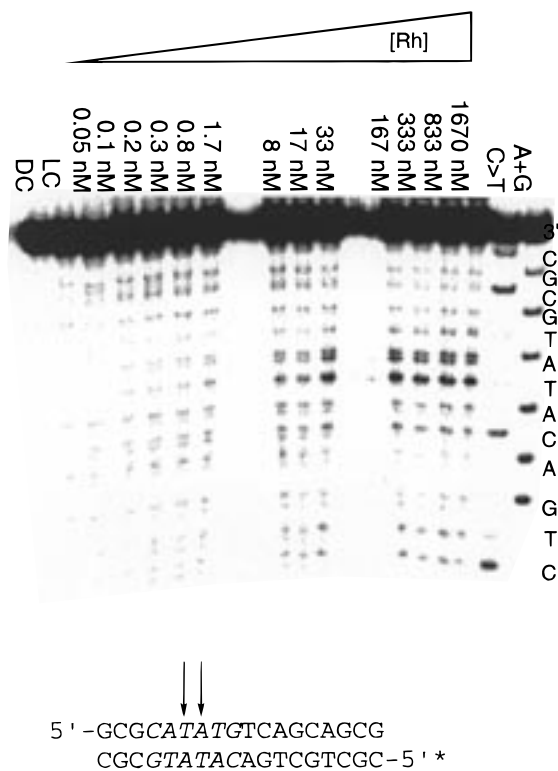


FIGURE 3: Photocleavage of 5'-³²P labeled target by Λ -1-Rh-(MGP)₂phi⁵⁺. The top of the gel shows the concentration of Rh used in each lane. Final duplex DNA concentrations were exactly 1 order of magnitude higher than the Rh concentrations for each irradiation reaction. Each sample was irradiated for 8 min at 313 nm. Maxam–Gilbert A + G and C > T sequencing lanes are shown to the far right. The buffer concentrations were 10 mM sodium cacodylate and 50 mM NaCl. Introduced target sites are shown in the sequence below the gel in italics and cleavage sites are indicated by arrows.

2 min on ice, followed by immediate 12000g, 10 min centrifugation of cellular debris. The pellet was discarded, and the lysate was treated with 10% polyethyleneimine to a final concentration of 0.5%. After 20 min of room-temperature incubation, the precipitated nucleic acids were spun down at 35000g for 25 min at 0 °C. Ammonium sulfate was then added to a concentration of 1.0 M and the solution was placed on ice for 30 min. The protein pellet was obtained by centrifugation at 35000g for 20 min and was redissolved into 10 mL of protein buffer at 0 °C. All remaining steps were performed at 4 °C. After filtration through a 0.22 μ M filter, this material was loaded onto a 5 mL Heparin column (Pharmacia), thoroughly rinsed with 100 mL of protein buffer. yAP-1 eluted at 700 mM NaCl on a continuous, linear 200 mL 0.01 to 2.00 M NaCl gradient with protein buffer as the FPLC carry buffer. The resultant material was >90% pure as visualized by gel electrophoresis and Coomassie Blue staining. This band was positive to Western antibody probes to both yAP-1 and thioredoxin, and highly active in DNA/protein gel retardation assays.

Photocleavage Reactions. Photocleavage reactions were performed using 5'-end-labeled oligonucleotides purified as described earlier. Cold carrier duplex was made using HPLC purified oligonucleotides. The photocleavage reactions contained 50 mM NaCl and 10 mM sodium cacodylate, pH 7.0, with a 10:1 ratio of DNA to rhodium complex. A 5 min preincubation in the dark was followed by 8 min irradiations

at 313 nm. Samples lacking metal complexes were irradiated for 15 min. Immediately after irradiation, each sample was frozen at -80 °C and lyophilized. They were resuspended in formamide loading buffer and directly run on a denaturing polyacrylamide sequencing gel (8 M urea and 20% polyacrylamide).

Competition Experiments to Measure Protein Binding. Metal complexes were freshly dissolved into doubly distilled, deionized water, and the concentrations of the stock solutions were determined by measuring absorbance ($\epsilon_{360} = 1.94 \times 10^4 \text{ M}^{-1} \text{ cm}^{-1}$). Protein concentrations were established by dilution from a stock dialyzed against protein buffer that had been quantitated by 280 nm absorbance to have 6.25 μ M protein. Each reaction had final concentrations as follows: 40 nM yAP-1, 2% Ficoll, 50 mM KCl, 25 nCurie of labeled oligonucleotide ($\sim 2 \text{ nM}$ final concentration of duplex DNA), 1 μ M bovine serum albumin as nonspecific carrier, and 15 mM Tris, pH 7.4. The amount of protein buffer included in the reaction varied among the experiments but never exceeded 2% of the final volume (v/v). The incubations were equilibrated for 3–6 h and were then loaded directly onto a running 5.5% native acrylamide gel buffered with 45 mM tris-borate buffer with 1 mM EDTA at pH 8.3. Order of incubation was varied and found to be unimportant. The electrophoresis was performed for 1 h at 100 V, after which the gels were vacuum-dried onto Whatman paper and exposed overnight to a Phosphorimager plate. Results were quantitated in ImageQuant, and data fitting was performed on Kaleidograph software, using the equation $\theta = 1 - (K_a)(\text{Rh}_T)/[1 + K_a(\text{Rh}_T)]$, where K_a is the association constant, Rh_T is the rhodium concentration, and θ is the fraction DNA bound (derived from equations in ref 33).

RESULTS

Purification of Recombinant Transcription Factor yAP-1. Previous investigations using recombinant yAP-1 relied on the activity of crude bacterial cell lysates of bacterial cells carrying the gene on a constitutively producing locus (30). Introduction of the *YAP1* gene to the pThioHis vector generated a thioredoxin/yAP-1 fusion protein. This fusion protein was additionally placed under the *lacZ* promoter, which allows controlled induction of protein expression in bacteria. The thioredoxin domain increased the temperature stability of yAP-1 so that the fusion protein was stable in protein buffer at 60 °C for up to 3 h with no discernible effect on DNA binding. Purifications from cell lysate by polyethyleneimine precipitation of cellular nucleic acids and a 25% ammonium sulfate cut yielded crude yAP-1 separation from the bulk of the cellular proteins. Finally, the use of a Heparin agarose affinity column resulted in >90% purity. As expected, gel shift assays showed that the addition of the thioredoxin fusion domain did not interfere with yAP-1 binding to oligonucleotides. Because of this maintenance of activity, combined with previous studies demonstrating the generally small perturbations introduced upon fusion of the thioredoxin domain (40), we used the fusion protein directly in assays. Additionally, this fusion generated a second epitope for antibody detection, so that the purification steps could be monitored with commercially available antibodies.

Design of Target Oligonucleotide. The contacts yAP-1 makes to the native AP-1 recognition element (ARE) have

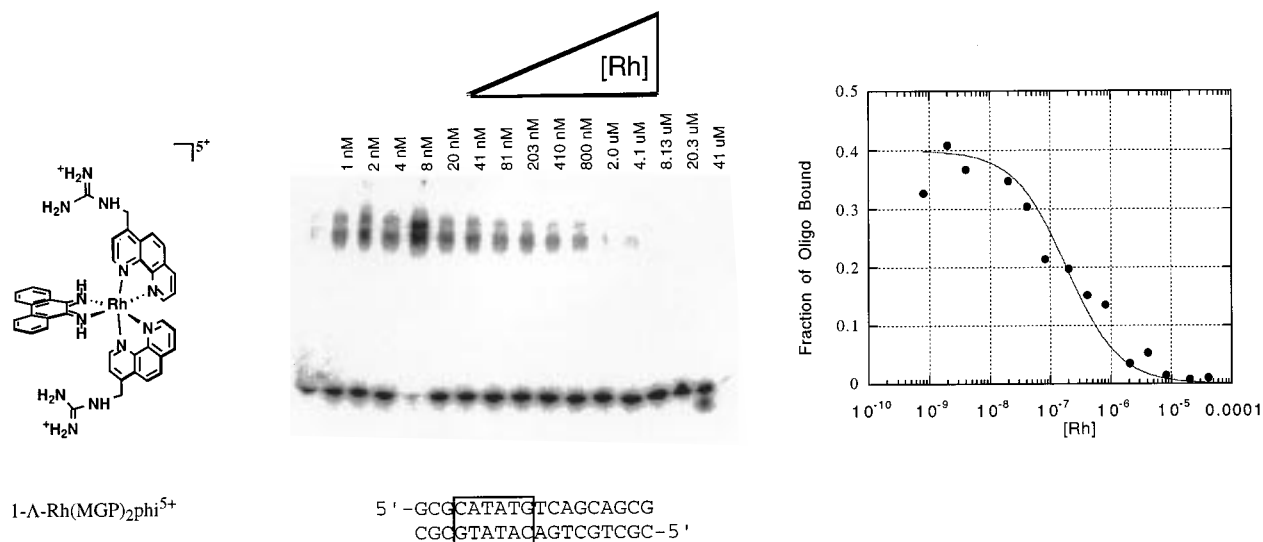


FIGURE 4: Competition between the protein yAP-1 and the metal complex $\Lambda-1\text{-Rh}(\text{MGP})_2\text{phi}^{5+}$ for the target oligonucleotide duplex as visualized by gel mobility retardation assay. To the left is shown the metal complex used in this experiment, below the center gel is shown the target oligonucleotide strand used in the competition reaction, and the graph to the right shows the quantitation and curve fit of the data. In this experiment, $\Lambda-1\text{-Rh}(\text{MGP})_2\text{phi}^{5+}$ competitively disrupts 50% of the yAP-1/DNA binding complexes at 120 nM concentration. Each 30 μL , 3 h incubation reaction contained, in addition to the concentration of metal complex indicated above each lane, 40 nM yAP-1, 2% Ficoll, 15 mM Tris, pH 7.4, 50 mM KCl, 25 nCurie $5'$ - ^{32}P -labeled target oligonucleotide duplex (2 nM DNA duplex), and 1 μM BSA. Competition reactions (10 μL of the 30 μL reaction) were directly loaded onto a running 5.5% nondenaturing polyacrylamide gel for 100 V h, and then visualized by Phosphorimager plates.

been well-characterized biochemically and are shown along with the target oligonucleotide in Figure 2 (30). To permit binding of $\Lambda-1\text{-Rh}(\text{MGP})_2\text{phi}^{5+}$ to a site also recognized by yAP-1, a minimum number of nucleotides not directly contacted by the protein were modified to introduce the recognition site preferred by the metal complex, 5'-CATATG-3'. The three base pair alterations needed to introduce 5'-CATATG-3' into the wild-type ARE removed only one AT base pair from the AT rich tract that dominates half the ARE, and inverted two others. yAP-1 interacts with both the modified sequence of the target oligonucleotide and the native sequence with a dissociation constant that is less than 5 nM (Figure S1, Supporting Information).

Recognition of Target Oligonucleotide by $\Lambda-1\text{-Rh}(\text{MGP})_2\text{phi}^{5+}$ as Visualized by Photocleavage. Having established strong interaction between the transcription factor and the target oligonucleotide sequence, DNA photocleavage studies were used to probe the interaction of the metal complexes and oligonucleotides used in this study. As in previous studies, the metal complexes were preequilibrated for 5 min with the oligonucleotide before irradiation to ensure equilibration (20); NMR studies indicate, however, that the equilibration is much more rapid (23). Upon irradiation, $\Lambda-1\text{-Rh}(\text{MGP})_2\text{phi}^{5+}$ exhibited strong recognition of the site introduced into the transcription promoter region (Figure 3) as seen through photocleavage. In contrast, very little cleavage was observed for wild-type ARE below micromolar concentrations (Figure S2, Supporting Information). As described previously, the cleavage seen is a strong doublet at the central AT step of the CATATG-binding site (13), consistent with the symmetric intercalation of the rhodium complex within its target site, as observed by NMR (23). We estimate a dissociation constant of 25 ± 10 nM by photocleavage titration at this doublet as a function of concentration based on curve fitting (see Materials and Methods). Photocleavage quantum yields for these metal

complexes are quite low (19), yet it is clear that binding saturation occurs well below 1 μM . The splitting of the 5' T into a double band is occasionally seen with photocleavage on small oligonucleotides with $\Lambda-1\text{-Rh}(\text{MGP})_2\text{phi}^{5+}$ (35). No specific sites of photocleavage activity in either oligonucleotide were observed for the metal complexes *rac*-Rh(phen) $_2\text{phi}^{3+}$ (data not shown) or $\Lambda-2\text{-Rh}(\text{MGP})_2\text{phi}^{5+}$ (Figure S3 and S4, Supporting Information) at concentrations lower than 10^{-5} M.

Isomer Specificity of Competition Between Metal Complexes and Target Oligonucleotide. Competition for the target oligonucleotide between yAP-1 and either $\Lambda-1\text{-Rh}(\text{MGP})_2\text{phi}^{5+}$ or $\Lambda-2\text{-Rh}(\text{MGP})_2\text{phi}^{5+}$ was examined by titrating with the metal complexes using gel retardation assays (Figures 4 and 5A). As standard procedure for all gel shift assays in our laboratory, reactions were loaded directed onto a running gel regardless of incubation time. Protein binding thus measured decreased in a sigmoidal fashion with increasing concentrations of the metal complex, albeit at different concentrations for different species of metal complex. Curve fitting of the ratios of the bound oligonucleotide to total oligonucleotide showed that the concentration of $\Lambda-1\text{-Rh}(\text{MGP})_2\text{phi}^{5+}$ required to reach half-dissociation of the protein-DNA sites was 118 nM (Figure 4). The complex $\Lambda-2\text{-Rh}(\text{MGP})_2\text{phi}^{5+}$, in contrast, showed no disruption of the DNA-protein complex at concentrations as high as 10 μM , but nonspecific aggregation of the DNA-protein complexes was evident at higher rhodium concentrations (Figure 5B). The aggregation did not occur until the metal complex was over 250 times more concentrated than yAP-1 in the binding reactions, and over 10 times higher in concentration than the nonspecific carrier protein BSA. This behavior was not seen with $\Lambda-1\text{-Rh}(\text{MGP})_2\text{phi}^{5+}$ at concentrations as high as 40 μM . The differential binding by $\Lambda-1\text{-Rh}(\text{MGP})_2\text{phi}^{5+}$ versus $\Lambda-2\text{-Rh}(\text{MGP})_2\text{phi}^{5+}$ clearly demonstrates isomer specificity in recognition by the metal complex

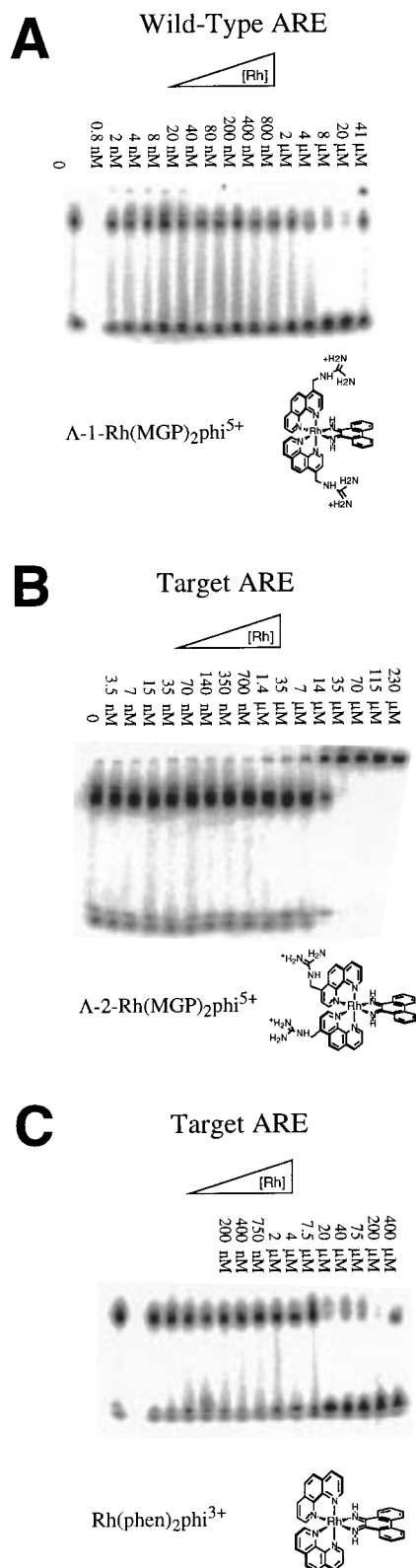


FIGURE 5: Control competition reactions for the protein yAP-1. (A) Λ -1-Rh(MGP)₂phi⁵⁺ with the wild-type ARE, (B) Λ -2-Rh(MGP)₂phi⁵⁺ with the target oligonucleotide, and (C) *rac*-Rh(phen)₂phi³⁺ with the target oligonucleotide. Competition between Λ -1-Rh(MGP)₂phi⁵⁺ and yAP-1 for the native ARE shows that it requires over 3 μ M of metal complex to compete effectively with the yAP-1 for an oligonucleotide that lacks the 5'-CATATG-3' binding region. Λ -2-Rh(MGP)₂phi⁵⁺ shows no competition for the protein/DNA complex, and *rac*-Rh(phen)₂phi³⁺ shows only sequence neutral competition above 10 μ M for *rac*-Rh(phen)₂phi³⁺. All gels were obtained with the conditions as in Figure 4.

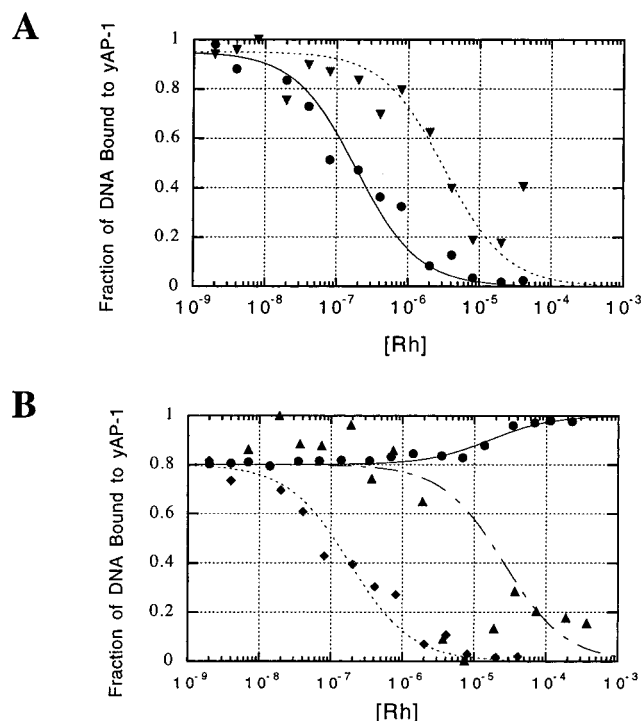


FIGURE 6: Comparison of fitted curves for competition between metal complexes and yAP-1. Gel shift assays were quantitated in ImageQuant, normalized, and then graphed and fitted in Kaleidograph. (A) Competition between yAP-1 and Λ -1-Rh(MGP)₂phi⁵⁺ for the target oligonucleotide (solid circles) and the wild-type oligonucleotide (inverted triangles). (B) The metal complexes Λ -1-Rh(MGP)₂phi⁵⁺ (diamonds), Λ -2-Rh(MGP)₂phi⁵⁺ (solid circles), and *rac*-Rh(phen)₂phi³⁺ (solid triangles) were used in competition experiments with yAP-1 for the target oligonucleotide.

(Figure 6B). The geometric repositioning of the pendant guanidiniums [e.g., Λ -1-Rh(MGP)₂phi⁵⁺ versus Λ -2-Rh(MGP)₂phi⁵⁺] increases by over 2 orders of magnitude the amount of metal complex needed to disrupt competitively specific protein-DNA complexes.

Binding reactions with the parent metal complex *rac*-Rh(phen)₂phi³⁺ were examined in similar competition experiments to explore the effect that a relatively sequence neutral intercalating metal complex has on yAP-1 and yAP-1/DNA complexes. *rac*-Rh(phen)₂phi³⁺ does not interfere with protein/DNA complexes directly, but competes at higher concentration sterically for sites in the major groove of the oligonucleotide (Figure 5C). Competition on both wild-type and target oligonucleotides had half-site occupancy at 23 μ M metal complex (Figure 6B). This value accurately reflects the lower overall binding affinity that *rac*-Rh(phen)₂phi³⁺, compared to Λ -1-Rh(MGP)₂phi⁵⁺, displays for DNA. Indeed, previous work has estimated the dissociation constant of this metal complex from DNA to be in the micromolar range (19), and photocleavage experiments with the native and target oligonucleotides described herein show no strong photocleavage bands at concentrations of metal complex up to 20 μ M.

Site-Specific Competition of yAP-1 and Λ -1-Rh(MGP)₂phi⁵⁺. To demonstrate that successful competition between yAP-1 and Λ -1-Rh(MGP)₂phi⁵⁺ for a DNA-binding site is dependent on the presence of a target 5'-CATATG-3' site, we performed identical competition experiments on both with the wild-type ARE oligonucleotide and with the target oligonucleotide. In these experiments, competition experi-

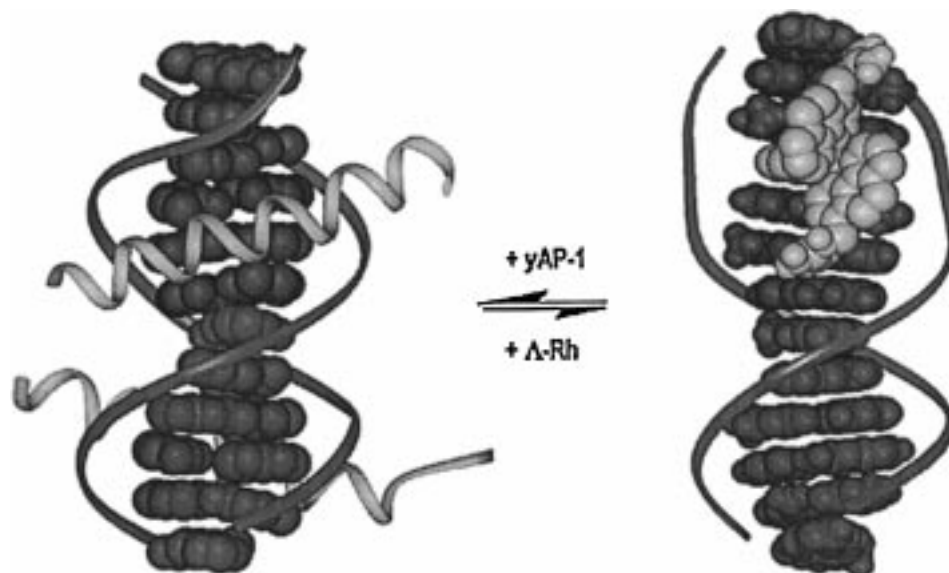


FIGURE 7: Schematic model of the competition between γ AP-1 and Δ -1-Rh(MGP) $_2$ phi $^{5+}$ on the target DNA. The models were constructed in InsightII based on NMR models of Δ -1-Rh(MGP) $_2$ phi $^{5+}$ intercalation at 5'-CATATG-3' sites (13) and the GCN4 crystal structure parameters (35). When occupied by the metal complex, the half site of the target site is unwound by 70° and sterically precludes protein association.

ments using an oligonucleotide lacking a binding site for Δ -1-Rh(MGP) $_2$ phi $^{5+}$ (as shown by photocleavage, see Supporting Information) was compared to experiments using the target oligonucleotide which contains the preferred binding site 5'-CATATG-3'. If Δ -1-Rh(MGP) $_2$ phi $^{5+}$ were nonspecifically interfering with the protein, identical behavior between these two different protein-DNA complexes would be expected. However, as seen in Figure 6A, Δ -1-Rh(MGP) $_2$ phi $^{5+}$ disrupted 50% of the protein-target DNA complexes at a concentration of 120 nM, whereas over 3 μ M rhodium was required to compete similarly on the wild-type oligonucleotide. This result represents an increase of 30 times the concentration of Δ -1-Rh(MGP) $_2$ phi $^{5+}$ required to disrupt γ AP-1-target oligonucleotide complexes (Figure 6A). In effect, the removal of the binding site from the oligonucleotide increases the concentration of metal complex required for successful competition with γ AP-1 by more than an order of magnitude.

DISCUSSION

Target Oligonucleotide Design. In general, the native ARE shows a great deal of tolerance for variation of the nucleotides within its binding site that are not closely contacted by the protein. However, attempts to introduce a metal complex binding site that disrupts one or more of the closely contacted base pairs resulted in a pronounced decrease in the binding affinity between γ AP-1 and the modified ARE (data not shown). Consistent with this notion, the mutation of the binding site to include a metal complex binding region without changing these essential base pairs, as shown in Figure 2, did not alter the binding of γ AP-1 to the oligonucleotide. Gel retardation assays showed that, at an approximate 2:1 molar ratio in titrations, the binding of the target oligonucleotide to the protein was quantitative at very low nanomolar concentrations (typically 8–10 nM of protein). Photocleavage with Δ -1-Rh(MGP) $_2$ phi $^{5+}$ confirmed that the metal complex strongly recognized the target oligonucleotide containing the three base pairs altered from the wild-type ARE.

Site Specificity of the Competition Reaction. The ability of a metal complex to compete specifically at low concentrations with a transcription factor for a promoter depends on the presence of an overlapping binding site for the two species. Competition between γ AP-1 and Δ -1-Rh(MGP) $_2$ phi $^{5+}$ for the target oligonucleotide showed disruption at concentrations more than an order of magnitude lower than seen for competition between the same species for the wild-type ARE. These controls show that the competitive disruption of the binding of γ AP-1 to the ARE depends on the specific DNA sequence and not on a nonspecific interaction with γ AP-1. Nonspecific interactions between Δ -1-Rh(MGP) $_2$ phi $^{5+}$ and the carrier BSA are also ruled out by the differential inhibition of γ AP-1 binding to DNA by Δ -1-Rh(MGP) $_2$ phi $^{5+}$. Interaction of the metal complex with BSA cannot account for the strongly sequence-specific competition between the transcription factor and Δ -1-Rh(MGP) $_2$ phi $^{5+}$ that occurs at concentrations of metal complex an order of magnitude below the concentration of BSA (Figure 6A).

There are pronounced differences in binding affinity for the two oligonucleotides and the metal complex Δ -1-Rh(MGP) $_2$ phi $^{5+}$, as seen both by photocleavage and by competition with γ AP-1 for an oligonucleotide. These differences show that the metal complex binding is specific to the sequence introduced into the ARE and not a nonspecific metal complex-protein interaction. The data furthermore show that the specific inhibition of protein binding is dependent on the presence of 5'-CATATG-3' within the promoter site.

Isomer and Complex Specificity of the Competition Reaction. The specificity in metal complex for Δ -1-Rh(MGP) $_2$ phi $^{5+}$ is demonstrated through the comparison between its competition reactions and those of related complexes. Other metal complexes showed nonspecific interference in the binding of γ AP-1 to the target oligonucleotide. Moreover, for other metal complexes the protein-promoter complex disruption was insensitive to the sequence of the DNA used. Both wild-type ARE and the target ARE show approximately the same

susceptibility to disruption, as is expected for a competition with metal that is not site specific. Furthermore, titrations revealed that only concentrations of Λ -1-Rh(phen)₂phi³⁺ above 20 μ M could disrupt DNA–protein complexes. These concentrations are well over 2 orders of magnitude greater than those seen for the specific competition of Λ -1-Rh(MGP)₂phi⁵⁺.

The symmetrical isomer Λ -2-Rh(MGP)₂phi⁵⁺ also showed no disruption of protein–DNA complexes up to 20 μ M either with the wild-type ARE or with the target ARE (Figure 6B). However, as the concentration of the metal complex increased to over 250 times that of yAP-1 and over 10 times that of the carrier BSA, aggregation in the wells occurred. Importantly, the only difference between this series of reactions and those performed for Λ -1-Rh(MGP)₂phi⁵⁺ was the orientation of the pendant guanidiniums. Positioning these arms so that they no longer contact DNA removes all specificity for DNA recognition, as seen previously (20). Inspection of the geometry of the two isomeric species (see Figure 1) shows that Λ -1-Rh(MGP)₂phi⁵⁺ directs its guanidinium functional groups into the DNA major groove. In contrast, Λ -2-Rh(MGP)₂phi⁵⁺ has both guanidiniums directed away from the intercalating phi ligand. The differences in orientation of hydrogen-bonding substituents between the two complexes must be the source of the different biochemical interactions of these metal complexes; indeed the overall charge on the complexes and thus their electrostatic interaction with DNA is the same. The proximity of the two guanidiniums in Λ -2-Rh(MGP)₂phi⁵⁺ could be responsible for the increased inter-complex contacts between multiple protein–DNA complexes we observe and, hence, cause a nonspecific aggregation not dissimilar to that used in ammonium sulfate precipitations of susceptible proteins in purification steps.

Model for Competition. yAP-1 shares many features with other bZIP transcription factors (36). Comparison of our designed target site with the related oligonucleotide site in the crystal structure of the GCN4 DNA-binding domain (37) suggests that the presence of a metal complex in the location of our introduced binding site would appear to block sterically one of the two dimer arms from making contacts with half of the semi-symmetrical core of the binding domain. All of the modifications to the ARE are located 5' to the pivotal G–C base pair, and hence on only one of the two dimer binding regions. Although there still exists some controversy regarding the dimerization and DNA binding pathway that proteins follow in vivo, recent models have suggested that bZIP proteins dimerize stepwise on some target sites of DNA (38, 39). The steric presence of a metal complex and the concomitant unwinding of half of the target site may also prevent the dimerization step of protein binding. Whatever the intervening species, the equilibrium between the protein and metal complex bound states on DNA and the probable DNA conformations are shown modeled in Figure 7.

Nature offers many parallels to the type of competition Λ -1-Rh(MGP)₂phi⁵⁺ shows with yAP-1. By using direct competition at overlapping sites, often two repressor proteins modulate gene expression. In much the same way, the site-specific competition between metal complexes and transcription factors might be exploited to modulate expression.

A Promising New Use for Metallointercalators. Octahedral metallointercalators would have to satisfy many criteria to be candidates for possible therapeutic applications. Perhaps the first of these important criteria would be the site-specific inhibition of a transcription factor binding to an enhancer site. We have shown previously that metal complexes can inhibit restriction endonucleases, and that metal complexes can mimic the binding characteristics of transcription factors (13, 40). We have now shown that a metallointercalator can compete directly with a transcription factor in the major groove for its target site. This is a fundamental first step toward controlling gene expression therapeutically using metallointercalators.

ACKNOWLEDGMENT

We also thank Dr. Christine Rener for technical assistance.

SUPPORTING INFORMATION AVAILABLE

Supporting data, which includes one two-part gel retardation experiment and three sequencing gels of photocleavage reactions and captions, is available. This material is available free of charge via the Internet at <http://pubs.acs.org>.

REFERENCES

- Ahmad, I., and Rao, D. N. (1996) *Crit. Rev. Biochem. Mol. Biol.* 31, 361–380.
- Donahue, B. A., Augot, M., Bellon, S. F., Treiber, D. K., Toney, J. H., Lippard, S. J., and Essigmann, J. M. (1990) *Biochemistry* 29, 5872–5880.
- Pil, P. M., and Lippard, S. J., (1992) *Science* 256, 234–237.
- Whitehead, J. P., and Lippard, S. J. (1996) *Metal Ions Biol. Sys.* 32, 687–726.
- Tomasz, M., and Palom, Y. (1997) *Pharm. Ther.* 76, 73–87.
- Poltev, V. I., Bruskov, V. I., Shulyupina, N. V., Rein, R., Shibata, M., Ornstein, R. L., and Miller, J. (1993) *Mol. Biol.* 27, 447–462.
- Denison, C., and Kodadek, T. (1998) *Chem. Biol.* 5, R129–R145.
- Liu, C. Smith, B. M., Ajito, K., Komatsu, H., GomezPaloma, L., Li, T. H., Theodorakis, E. A., Nicolau, K. C., and Vogt, P. K. (1996) *Proc. Natl. Acad. Sci. U.S.A.* 93, 940–944.
- Nicolaou, K., Tsay, S. C., Suzukit, T., and Joyce, G. F. (1992)-*J. Am. Chem. Soc.* 114, 7555–7557.
- Nicolaou, K., and Dai, W. (1991) *Angew. Chem.* 30, 1387–1416.
- Wemmer, D. E., and Dervan, P. B. (1997) *Curr. Opin. Struct. Biol.* 7, 355–361.
- Gottesfeld, J., Neely, L., Trauger, J. W., Baird, E. E., and Dervan, P. B. (1997) *Nature* 387, 202.
- Terbrueggen, R. H., and Barton, J. K. (1995) *Biochemistry* 34, 8227–8234.
- Johann, T. W., and Barton, J. K. (1996) *Philos. Trans. R. Soc. London A* 354, 299–324.
- Hudson, B. P., and Barton, J. K. (1998) *J. Am. Chem. Soc.* 120, 6877–6888.
- David, S. S., and Barton, J. K. (1993) *J. Am. Chem. Soc.* 115, 2984–2985.
- Shields, T. P., and Barton, J. K. (1995) *Biochemistry* 34, 15049–15056.
- Krotz, A. H., Hudson, B. P., and Barton, J. K., (1993) *J. Am. Chem. Soc.* 115, 12577–12578.
- Sitlani, A., Long, E. C. Pyle, A. M., and Barton, J. K. (1992) *J. Am. Chem. Soc.* 114, 2303–2312.
- Terbrueggen, R. H., Johann, T. W., and Barton, J. K. (1998) *Inorg. Chem.* 37, 6874–6883.
- Campisi, D., Morii, T., and Barton, J. K. (1994) *Biochemistry* 33, 4130–4139.

22. Pabo, C. O., and Sauer, R. T. (1992) *Annu. Rev. Biochem.* 61, 1053.
23. Franklin, S. J., and Barton, J. K. (1998) *Biochemistry* 37, 16093–16105.
24. Kim, J. L., Nikolov, D. B., and Burley, S. K. (1993) *Nature* 365, 520–527.
25. Kim, Y. C., Geiger, J. H., Hahn, S., and Sigler, P. B. (1993) *Nature* 365, 512–520.
26. O Shea, E. K., Klemm, J. D., Kim, P. S., and Alber, T. (1991) *Science* 254, 539–544.
27. Moye-Rowley, W. S., Harshman, K. D., and Parker, C. S. (1988) *Cold Spring Harbor Symp. Quant. Biol.* LIII, 711.
28. Moye-Rowley, W. S., Harshman, K. D., and Parker, C. (1989) *Genes Dev.* 3, 283–292; unpublished results in the Parker lab.
29. Wemmie, J., Wu, A.-L., Harshman, K. D., Parker, C. S., and Moye-Rowley, W. (1994) *J. Biol. Chem.* 269, 14690.
30. Harshman, K. D., Moye-Rowley, W. S., and Parker, C. (1988) *Cell* 53, 321–330.
31. Chow, C. S., and Barton, J. K. (1992) *Methods Enzymol.* 212, 219–242.
32. Kunkel, T. A. (1985) *Proc. Natl. Acad. Sci. U.S.A.* 82, 488–492.
33. Singleton, S., and Dervan, P. B. (1992) *J. Am. Chem. Soc.* 114, 6957.
34. LaValle, E. R., DiBlasio, E. A., Kovacic, S., Grant, K. L., Schendel, P. F., and McCoy, J. M. (1993) *BioTechnology* 11, 187–193.
35. Johann, T. W. California Institute of Technology, Ph.D. Dissertation.
36. Vinson, C. R., Sigler, P. B., and McKnight, S. (1989) *Science* 246, 911.
37. Ellenberger, T. E., Brandl, C. J., Struhl, K., and Harrison, S. C. (1992) *Cell* 71, 1223–1237.
38. Metallo, S. J., and Schepartz, A. (1997) *Nat. Struct. Biol.* 4, 115–117.
39. Weiss, M. A. (1990) *Biochemistry* 29, 8020–8024.
40. Sitlani, A., Dupureur, C. M., and Barton, J. K. (1993) *J. Am. Chem. Soc.* 115, 12589–12590.

BI9827969